

Characterization of the Chemical Reactivity and Selectivity of DNA Bases Through the Use of DFT-Based Descriptors

Vanessa Labet, Christophe Morell, Vincent Tognetti, Olga A. Syzgantseva, Laurent Joubert, Nelly Jorge, André Grand, and Jean Cadet

Contents

1	Introduction	36
2	Theoretical Framework	38
2.1	Conceptual DFT Framework	38
2.2	Global Descriptions	40
2.3	Local and Nonlocal Descriptors	42
2.4	Selectivity Descriptors for Excited States	44
3	Application: Reactivity of Nucleic Acid Bases	46
3.1	Introduction	46
3.2	Reactivity Descriptors Computed for Isolated Nucleobases	47
3.3	Structural Features of DNA	53
3.4	Reactivity Differences Between the Nucleobases	55
4	Conclusions	67
	References	67

V. Labet

Sorbonne Universités, UPMC Univ Paris 6, MONARIS, UMR 8233, 75005 Paris, France

C. Morell (✉)

Université de Lyon 1, ISA, UMR 5280, 5 rue de la Doua, 69100 Villeurbanne, France

e-mail: Christophe.morell@univ-lyon1.fr

V. Tognetti • O.A. Syzgantseva • L. Joubert

Normandie Université, COBRA, UMR6014 & FR 3038, Université de Rouen, INSA Rouen, CNRS, 1 rue Tesnière, 76821 Mont-Saint-Aignan Cedex, France

N. Jorge

Área Fisicoquímica, Facultad de Ciencias Exactas y Naturales y Agrimensura, UNNE, Campus Universitario, Av. Libertad 5400, (3400), Corrientes, Argentina

A. Grand • J. Cadet

CEA Grenoble -Institut Nanosciences et Cryogénie/SCIB/LAN (UMR-E n 3 CEA-UJF), CEA-Grenoble, 17, rue des Martyrs, 38054 Grenoble Cedex 9, France

Abstract In this chapter, the use of conceptual DFT descriptors for understanding the occurrence and likely mechanisms of formation of DNA lesions is reviewed. After a synthetic presentation of the principal DFT-based descriptors, the global reactivity and selectivity of DNA bases are investigated from global and local descriptors. Then, the formation of several DNA lesions is studied including cytosine compound deamination, intra-strand DNA cross-links, and pyrimidine dimer photoproducts. It appears from the use of the global and local DFT-based descriptors that most of the experimental facts can be theoretically rationalized.

Keywords Descriptors of chemical reactivity • Conceptual DFT • DNA damage • Cytosine deamination • Cyclobutane pyrimidine dimers • Pyrimidine (6–4) pyrimidone photoproducts • Tandem base lesions • Purine 5',8-cyclonucleosides • Dual descriptors

1 Introduction

Deoxyribonucleic acid (DNA) in its cellular environment is prone to a wide range of degradation pathways involving hydrolysis and reactions with various chemicals and physical agents [1, 2]. One of the two main hydrolytic reactions involving DNA leads to the cleavage of the *N*-glycosidic bond of 2'-deoxyribonucleosides, preferentially at guanine (Gua) and to a lesser extent at adenine (Ade) sites with subsequent formation of highly mutagenic abasic sites [3]. Purine bases are also subject to deamination as well as cytosine (Cyt) and 5-methylcytosine (5-MeCyt) [1, 2], the fifth nucleobase [4] that has recently received major attention due to its strong implication in epigenetic pathways [5] through enzymatic oxidation of the 5-methyl group of the pyrimidine ring [6, 7].

Early evidence has shown that the susceptibility of the nucleobases to hydrolytic deamination decreases for model compounds in the following order: Cyt > 5-MeCyt > purine bases [8–10]. It is worth noting that uracil (Ura) and thymine (Thy), the two main bases thus hydrolytically generated, are efficiently removed from DNA by uracil and thymine DNA glycosylases respectively, two mismatch repair enzymes [11, 12]. Other important endogenous reactions to cellular DNA are mediated by reactive oxygen species (ROS), actually mostly by hydroxyl radical ($\cdot\text{OH}$) that efficiently reacts indistinctively with neighboring molecules at the site where it is generated [13].

The initial event of the pathway leading to cellular DNA oxidation is mono-electronic reduction of dioxygen (O_2) during mitochondrial respiration [14], inflammation [15], or phagocytosis [16] giving rise to an unreactive superoxide anion radical ($\text{O}_2^{\cdot-}$) [13]. Dismutation of $\text{O}_2^{\cdot-}$ leads to low reactive H_2O_2 that is able to migrate through the cells before eventually being reduced by transition metals such as Fe^{2+} ions and converted into highly reactive $\cdot\text{OH}$. A large body of

information is now available on the reaction of $\cdot\text{OH}$ with nucleobases [17, 18] and 2-deoxyribose [17, 19, 20] in terms of reactivity, mechanisms involved, and oxidation products. Thus more than 100 oxidatively generated modifications including single and tandem base lesions together with oxidized sugar residues have been characterized in model compounds [17–20]. It may be added that almost 20 modified nucleosides have been accurately measured in cellular DNA, mostly by using high-performance liquid chromatography (HPLC) coupled with either tandem mass spectrometry (MS/MS) or MS^3 experiments [21].

Carbonate anion radical ($\text{CO}_3^{\cdot-}$), another powerful oxidant, may be generated during inflammation through, in the initial step, recombination of $\text{O}_2^{\cdot-}$ and nitrite oxide ($\cdot\text{NO}$), the product of NO synthase [22]. Subsequent reaction of peroxynitrite thus formed with CO_2 gives rise to unstable nitrosoperoxycarbonate that decomposes with simultaneous release of $\text{CO}_3^{\cdot-}$ and nitrating $\cdot\text{NO}_2$ [23, 24]. $\text{CO}_3^{\cdot-}$ is able to selectively one-electron-oxidize guanine [25], producing a related radical cation that efficiently reacts with nucleophiles generating a variety of damage including single lesions, intra- and inter-strand DNA cross-links, and DNA-protein adducts [19, 26–28].

Numerous exogenous agents are also able to oxidize DNA either directly or after metabolic activation. It is well documented that ionizing radiation generates $\cdot\text{OH}$ through radiolysis of water molecules and ionize DNA components via indirect and direct effects, respectively [17]. Other relevant oxidizing agents include endogenous and exogenous photosensitizers that may act as one-electron oxidants (type I photosensitization mechanism) and/or generators of singlet oxygen (type II photosensitization mechanism) [29, 30], another important ROS that selectively reacts with guanine [27]. The main important genotoxic effects of solar radiation on human skin are explained in terms of direct excitation of nucleobases by the UV components including mostly the more energetic UVB photons and to a lesser extent UVA radiation [31, 32]. An excited pyrimidine base is able to react with vicinal thymine or cytosine via two competitive photoreactions whose efficiency is strongly primary sequence dependent. The formation of *cis-syn* cyclobutane pyrimidine dimers (CPDs) involves a [2+2] photocycloaddition reaction, whereas competitive Paternò-Büchi photocycloaddition gives rise to pyrimidine (6–4) pyrimidone photoproducts (6–4PPs) through either a dioxetane or an azetidine intermediate [32]. Photoisomerization of the UVB-induced 6–4PPs into related Dewar valence isomers has been shown to imply mostly UVA radiation in cellular DNA [33].

The base modifications generated to cellular DNA by deamination, oxidants, or photochemical reactions are usually removed from double-stranded DNA either by base excision repair for single lesions [34] or nucleotide excision repair for bulky DNA damage such as CPDs and 6–4PPs [35–37]. However, if DNA replication occurs before repair of the modifications, there is a risk of mutation induction in the newly synthesized DNA strand when the damage is miscoding [38]. This may lead to deleterious effects including long-term occurrence of carcinogenesis as the result of incorrect processing of cytosine-containing CPDs that are likely to undergo deamination [37]. This explains why numerous and extensive investigations have

been devoted to the characterization, measurement, and biological assessment (repair, mutagenic potential) of DNA lesions.

More recently, major efforts have been made to complement the above information by using theoretical approaches for gaining further insights into the chemical reactivity of the bases. In the present chapter, emphasis is placed on the critical review of information gained from the use of density functional theory-based descriptors that shed new light on the endogenous and exogenous formation of several single and tandem lesions. Deamination of unsaturated and 5,6-saturated cytosine compounds that involves tautomerization reaction is first considered. In addition three main types of DNA modifications are reviewed. Two involve radical reactions initiated by $\cdot\text{OH}$ that lead to the formation of tandem base lesions between two adjacent thymine-purine bases [19, 39] and cross-links between the 2-deoxyribose from the intramolecular cyclization of C5' radical to either adenine or guanine at C8 [40, 41]. Lastly the relevance of DFT descriptors for investigating the reactivity of excited pyrimidine bases has been challenged through consideration of the relative formation of CPDs and 6-4PPs, the main UVB-induced bipyrimidine photoproducts [32].

2 Theoretical Framework

It is a chemical fact that some molecules are more stable and others more reactive. It is also often observed that some atomic positions within molecules are more prone to react than their neighbors. Different chemical theories have the ambition to rationalize these experimental facts. The most fruitful and elegant framework so far is certainly the density functional theory of chemical reactivity, also called conceptual DFT [42, 43]. Conceptual DFT is a subfield of DFT in which one tries to extract from the electron density relevant concepts and principles that help us to understand and predict the chemical behavior of a molecule. The aim of this section is to briefly present the chemical descriptors used in the chapter and the way they are usually computed.

First an overall picture of the theoretical framework is depicted and discussed. Section 2.2 gives an introduction to global indexes such as chemical potential and chemical hardness. In Sect. 2.3 the local counterparts of the global descriptors are presented. The last section is dedicated to the extension of the local reactivity descriptor, called dual descriptor, to photoexcited biomolecules.

2.1 Conceptual DFT Framework

Density functional theory is original in the sense that within the DFT framework, a molecule is considered as an electron density stabilized and shaped by the electric field created by nuclei. In other words, in DFT a molecule is seen as a whole and not

as a collection of atoms. This way of considering a molecule simplifies the modeling of chemical processes. During a reaction, the molecular system undergoes either a loss or a gain of electrons or both and a relocation of the nuclei. These modifications of the molecular structure can be monitored through the successive responses of the energy with respect to the variation of the number of electrons and to the modification of the external potential [44].

$$\begin{aligned}
 d\mathcal{E} = & \left(\frac{\partial \mathcal{E}}{\partial N} \right)_v dN + \int \left[\frac{\delta \mathcal{E}}{\delta v(r)} \right]_N dv(r) dr \\
 & + \frac{1}{2} \left(\frac{\partial^2 \mathcal{E}}{\partial N^2} \right)_v dN^2 + dN \int \left[\frac{\delta^2 \mathcal{E}}{\partial N \delta v(r)} \right] dv(r) dr + \frac{1}{2} \iint \left[\frac{\delta^2 \mathcal{E}}{\delta v(r) \delta v(r')} \right]_N dv(r) dv(r') dr dr' \\
 & + \frac{1}{6} \left(\frac{\partial^3 \mathcal{E}}{\partial N^3} \right)_v dN^3 + \frac{1}{3} dN^2 \int \left[\frac{\delta^3 \mathcal{E}}{\partial^2 N \delta v(r)} \right] dv(r) dr + \dots \dots \dots
 \end{aligned}
 \tag{1}$$

Interestingly, each and every derivative of the energy within this framework has a chemical meaning generally related to a property already in use by theoreticians and experimentalists. The identification of the first derivative of the energy with respect to the number of electrons to the opposite of the electronegativity exemplifies this statement. It is worth noticing that three sets of derivatives exist. Derivatives with respect to the number of electrons give rise to global descriptors. Their values are the same wherever position they are calculated. The global descriptors measure the chemical reactivity of the system as a whole. The responses of the energy with respect to the external potential are local descriptors and constitute the second set of indexes. Their values are dependent on the position where they are evaluated. These indexes probe the chemical selectivity of the system. Generally, positions exhibiting the highest values of a local descriptor are more prone to react than positions exhibiting the lowest values. Finally, second derivatives with respect to the external potential give rise to nonlocal responses [45]. The values of this kind of descriptors depend on two sets of spatial variables, and they are likely related to the polarization of the system. Table 1 summarizes the names and definitions of the main global and local descriptors. The chemical relevance of the last two entries of Table 1 has not yet been investigated. As a consequence, they have not been named and will not be considered further in this chapter.

The two next sections detail the mathematical definition and chemical meaning of these indexes.

Table 1 Summary of global and local descriptors as energy derivatives

Derivative order	Mathematical definition	Name
0	$\mathcal{E}[N, v] = \mathcal{E}_{elec}[\rho]$	Energy
1	$\left(\frac{\partial \mathcal{E}}{\partial N}\right)_v = \mu$	Chemical potential [46]
	$\left(\frac{\delta \mathcal{E}}{\delta v(r)}\right)_N = \rho(r)$	Electron density
2	$\left(\frac{\partial^2 \mathcal{E}}{\partial N^2}\right)_v = \eta$	Chemical hardness [47]
	$\left(\frac{\delta^2 \mathcal{E}}{\partial N \delta v(r)}\right) = f(r)$	Fukui function [48]
	$\left(\frac{\delta^2 \mathcal{E}}{\delta v(r) \delta v(r')} \right)_N = \chi_1(r, r')$	Linear response [49]
3	$\left(\frac{\partial^3 \mathcal{E}}{\partial N^3}\right)_v = \left(\frac{\partial \eta}{\partial N}\right)_v = \gamma$	Hyper-hardness [50, 51]
	$\left(\frac{\delta^3 \mathcal{E}}{\partial^2 N \delta v(r)}\right) = \left(\frac{\partial f(r)}{\partial N}\right)_v = \left(\frac{\delta \eta}{\delta v(r)}\right)_N = f^{(2)}(r)$	Dual descriptor [50]
	$\left(\frac{\delta^3 \mathcal{E}}{\partial N \delta v(r) \delta v(r')}\right) = \left(\frac{\partial \chi(r, r')}{\partial N}\right)_v = \left(\frac{\delta f(r)}{\delta v(r')}\right)_N = \xi(r, r')$	
	$\left(\frac{\delta^3 \mathcal{E}}{\delta v(r'') \delta v(r') \delta v(r)}\right)_N = \left(\frac{\delta \xi(r, r')}{\delta v(r'')}\right)_N = \chi_2(r, r', r'')$	

2.2 Global Descriptions

As already mentioned in the previous section, global DFT-based descriptors connect the electronic features to the reactivity of the system. The very basis of conceptual DFT has been the identification of the first derivative of the energy with respect to the number of electrons (called chemical potential for obvious reasons) to the opposite of the electronegativity as it has been proposed by Iczkowski and Margrave [46, 52]:

$$\left(\frac{\partial \mathcal{E}}{\partial N}\right)_v = \mu \quad (2)$$

Using the finite difference approximation, the chemical potential can be computed as

$$\mu \approx -\frac{1}{2}(I + A) \quad (3)$$

In Eq. 3, I and A respectively stand for the vertical ionization potential and the electron affinity. This working equation shows how the chemical potential is connected to Mulliken [53] electronegativity. By adding a second layer of approximation, based upon the Koopmans' theorem, one gets

$$\mu \approx \frac{1}{2}(\epsilon_{\text{LUMO}}[\text{N}, \text{v}] + \epsilon_{\text{HOMO}}[\text{N}, \text{v}]) \quad (4)$$

where ϵ_{LUMO} and ϵ_{HOMO} are the energies of the lowest unoccupied molecular orbital (LUMO) and the highest occupied molecular orbital (HOMO). Just like the electronegativity, the chemical potential evaluates the escaping tendency of the electrons.

Another great achievement of conceptual DFT was the proposal by Parr and Pearson [47] to measure the chemical hardness (concept introduced by the very same Pearson in the 1960s) using the second N-derivative:

$$\left(\frac{\partial^2 \mathcal{E}}{\partial N^2}\right)_{\text{v}} = \eta \quad (5)$$

Softness [54] has been naturally defined as the hardness inverse ($S = 1/\eta$). Chemical hardness is a versatile concept upon which two quite important principles are built. Originally, chemical hardness has been designed to rationalize the outcome of Lewis acid-base reactions. As stated by Pearson [55], hard acids prefer to bind hard bases, and soft bases preferentially react with soft acids. This statement is the basis of the hard and soft acids and bases principle. As 90 % of the chemical reactions belong into this heading, the HSAB principle proved itself quite handy. Later considerations by Pearson led to believe that hardness is also a strong indicator of chemical stability. The maximum hardness principle [56, 57] that states that molecules tend to be as hard as possible is the consequence of the evolution of the concept.

Later on, another index built upon the chemical potential and the chemical hardness has been proposed to describe the electrophilicity of a system. The chemical potential, as first N-derivative, must be negative for an electronically stable system. Indeed, a positive chemical potential would lead to an autoionization of the system that would lower its energy. Since the chemical potential is always negative, all systems are considered as electrophile and their energies decrease as they acquire electrons. In a seminal publication, Parr and coworkers [58] have shown that the maximum number of electrons a system can acquire is given by

$$\Delta N = -\frac{\mu}{\eta} \quad (6)$$

The lowering in energy is

$$\Delta \mathcal{E} = -\frac{\mu^2}{2\eta} \quad (7)$$

The electrophilicity index has been defined as

$$\omega = \frac{\mu^2}{2\eta} \quad (8)$$

The higher the value of this descriptor, the more electrophilic the system is.

2.3 Local and Nonlocal Descriptors

Besides global indexes, several local indexes have been defined as derivatives of the energy with respect to the external potential. Those descriptors whose values are dependent on the position they are evaluated ascribe the selectivity of atomic sites. In most cases, three different kinds of energies can control the selectivity of a chemical process, namely, electrostatic, frontier, and polarization interactions [59, 60]. Each local index happens to describe the corresponding local response.

The first v -derivative is the electron density, which enters the integral describing electrostatic interactions:

$$\left(\frac{\delta \mathcal{E}}{\delta v(r)} \right)_N = \rho(r) \quad (9)$$

Two kinds of second derivatives of the energy including the crossed N, v -derivative of the energy and the second v -derivative can be defined. The crossed derivative has been named Fukui function [48] after Kenichi Fukui, the founder of frontier molecular orbital theory [61, 62]. This function can be roughly approximated by the density of the frontier orbitals HOMO and LUMO.

$$\left(\frac{\delta^2 \mathcal{E}}{\delta v(r) \partial N} \right) = \left(\frac{\partial \rho(r)}{\partial N} \right)_v = f(r) \quad (10)$$

This quantity can be seen as the distribution function of one electron gained or lost over the system. To really get these two kinds of information, the right and left derivatives have been actually used. They are called electrophilic/nucleophilic Fukui functions [63] (f^+ and f^-):

$$\left(\frac{\partial \rho(r)}{\partial N} \right)_v^{+/-} = f^{+/-}(r) \quad (11)$$

From this function the actual location of the charge transfer can be monitored. Fukui function has been widely used in the last two decades to predict and rationalize the regioselectivity or regiospecificity of chemical processes [64–67].

The second v -derivative of the energy is the linear response function [68, 69]:

$$\left(\frac{\delta^2 \mathcal{E}}{\delta v(r) \delta v(r')} \right) = \left(\frac{\delta \rho(r)}{\delta v(r')} \right)_v = \chi(r, r') \quad (12)$$

This function describes how the electron density is modified at point r' when the external potential is changed at position r . Descriptors that depend on more than one set of coordinates are called nonlocal. This function is symmetrical with respect to the exchange of coordinates. The computation of the latter quantity is quite cumbersome. Besides, the chemical understanding of a function that depends on two sets of coordinates is quite difficult. It is therefore easily understandable that this function has been scarcely used so far. However, its usefulness in the rationalization of inductive and mesomeric effects [70] came out lately.

The last local descriptor presented here is the dual descriptor [71, 72], also known as second-order Fukui function. This index has been introduced in 2005 to predict whether an atomic site within a molecule is more electrophilic than nucleophilic or the other way around. The definition of the dual descriptor, symbolized by $\Delta f(r)$ or $f^{(2)}(r)$, as the third derivative of the energy is not very meaningful:

$$\left(\frac{\delta^3 \mathcal{E}}{\delta^2 N \delta v(r)} \right) = f^{(2)}(r) = \Delta f(r) \quad (13)$$

An alternative and more useful definition is

$$\left(\frac{\partial^2 \rho(r)}{\partial N^2} \right)_v = \Delta f(r) \quad (14)$$

Using the finite difference approximation and the Koopmans' theorem, the dual descriptor can be computed through

$$\left(\frac{\partial^2 \rho(r)}{\partial N^2} \right)_v \approx f^+(r) - f^-(r) \approx \rho_{LUMO}(r) - \rho_{HOMO}(r) \quad (15)$$

From this working definition, it is plain that the sign of this descriptor describes the philicity of a molecular site. Positions with positive values of dual descriptor are more electrophilic than nucleophilic. The density of the LUMO at this location is higher than that of the HOMO. On the contrary, positions with negative values of dual descriptor are more nucleophilic than electrophilic. In this case, at those locations, the density of the HOMO is higher than that of the LUMO. This descriptor has proved quite useful to rationalize both the regioselectivity and the regiospecificity of chemical processes.

It is quite important to point out that local reactivity indexes described so far are not suited for a comparison between species. To perform these kinds of studies, one needs to combine selectivity and reactivity information. Thus several indexes have been designed to help rationalize the reactivity difference of the same atomic site

within a molecular family. Historically, the first descriptor proposed was the local softness [73]:

$$s(r) = \left(\frac{\partial \rho(r)}{\partial \mu} \right)_v = \left(\frac{\partial \rho(r)}{\partial N} \right)_v \left(\frac{\partial N}{\partial \mu} \right)_v = \frac{f(r)}{\eta} \quad (16)$$

Obviously, the local softness contains the same information about selectivity as the Fukui function. Local softness also contains additional information about the global reactivity of the molecule. Combined, these pieces of information allow making a comparison between molecules.

More recently, using a similar line of arguments, the grand canonical dual descriptor (GCDD), symbolized by $\Delta s(r)$ or $s^{(2)}(r)$, has been developed [74]:

$$s^{(2)}(r) = \Delta s(r) = \left(\frac{\partial s(r)}{\partial \mu} \right)_v = \frac{\partial}{\partial \mu} \left(\frac{f(r)}{\eta} \right)_v = \frac{\Delta f(r)}{\eta^2} - \frac{f(r)}{\eta^3} \left\{ \frac{\partial \eta}{\partial N} \right\} \quad (17)$$

As the derivative of the chemical hardness with respect to the electron number is supposedly negligible, the GCDD is generally assessed through

$$s^{(2)}(r) = \Delta s(r) \approx \frac{\Delta f(r)}{\eta^2} \quad (18)$$

2.4 Selectivity Descriptors for Excited States

Descriptors presented in the previous section characterize either the reactivity or the selectivity for chemical processes that occur in the ground state. A recent extension of conceptual DFT has been proposed to tackle the selectivity of excited species [75, 76]. Basically, when an electronic system is excited by an electromagnetic field, its electron density is distorted. The main assumption is that the predominant process is the relaxation of the density (geometrical relaxation is overlooked). Mathematically, the whole extension is based upon a singularity of density functional theory. Indeed for whatever excited state, the electronic chemical potential is no longer a global quantity but on the contrary a local quantity. This property is due to the fact that the electron density of an excited species is not stationary. In other words, the excited electron density is not an optimum of the electron density functional. Translated into mathematics, this property reads

$$\left(\frac{\delta \mathcal{E}[\rho_i]}{\delta \rho(r)} \right)_v = \mu_i(r) \quad (19)$$

in which ρ_i is the density of the i th excited state. When the energy is computed using the true ground state electron density, Eq. 19 becomes

$$\left(\frac{\delta\mathcal{E}[\rho_0]}{\delta\rho(r)}\right)_v = \left(\frac{\partial\mathcal{E}[\rho_0]}{\partial N}\right)_v = \mu \equiv Cst \quad (20)$$

The chemical potential has then the same value anywhere within the molecular volume, noted Cst in Eq. 20. The minimization of the integral form of Eq. 19 provides an excellent descriptor of the chemical behavior of atomic site within the molecule:

$$\delta\mathcal{E} = \int_{\rho_i \rightarrow \rho_0} \mu_i(r) \delta\rho(r) dr \quad (21)$$

Indeed, for this equation to be minimum, it is obvious that positions with high values of the local chemical potential are depleted during the relaxation process, while positions with low values of the local chemical potential gain electron density. To reformulate this statement, it can be established that during the relaxation process from the excited state to the ground state, an intramolecular electron flux appears driven by the opposite of the gradient of the local chemical potential. The main assumption upon which the whole development is based is that the physical relaxation can be induced by a chemical partner. Following this line, an electrophile would attack positions which are depleted during the density relaxation. On the other hand, a nucleophile would attack locations that gain electron density during the relaxation. If one is capable of getting an analytical expression of the local chemical potential, one can monitor the electron flux and get a chemical picture of the selectivity of excited species. From the basics of DFT, it is well known that

$$\mu_i(r) = v(r) + \frac{\delta F[\rho_i]}{\delta\rho(r)} \quad (22)$$

in which $F[\rho]$ is the Hohenberg-Kohn universal functional.

The next step is to assume that the excited density can be written as a distortion of the ground state density. Then, using a Taylor expansion, one gets after several cumbersome approximations the following expression:

$$\mu_i(r) \approx \mu_0 + \int \frac{\delta_0^i \rho(r')}{|r - r'|} dr' \quad (23)$$

Specifically, for the first excited state, the quantity $\delta_0^i \rho(r)$ has very recently been defined as the first-order state-specific dual descriptor [77]. It can be approximated by the difference between the densities of the LUMO and the HOMO and therefore is very similar to the usual dual descriptor defined in Sect. 2.3. Therefore, the second term of the right-hand side of Eq. 23 can be seen as an electrostatic potential created by the dual descriptor density. This potential constitutes the local response and has been called dual potential ($V^{\Delta f}$). It is quite straightforward to show that the

Table 2 Chemical behavior for the ground state and the first excited state

Ground state $\Delta f(r)$		Excited state $\delta_0^1 \rho(r')$		Interactions
Sign	Character	Sign	Character	
+	Electrophilic	+	Nucleophilic	Favorable
–	Nucleophilic	–	Electrophilic	Favorable
+/–	el/nu	–/+	el/nu	Unfavorable

sign of this dual potential has a chemical meaning opposite to that of the dual descriptor for the ground state. As a consequence, the best interaction between two species, one of which being excited, is given in Table 2.

From these sets of descriptors, most of the chemical reactivity and selectivity can be explained. The next section is dedicated to the use of these indexes for the rationalization of the formation of several DNA lesions.

3 Application: Reactivity of Nucleic Acid Bases

3.1 Introduction

DNA, though responsible for carrying the genetic information, is characterized by some chemical instability; this may be particularly important when cellular DNA is exposed to external aggressions but also occurs under physiological conditions [1]. DNA is damaged continuously and, hopefully, in most cases efficiently repaired. Nonetheless, when repair is deficient, or if DNA replication takes place (mitosis) before repair is achieved, mutation may occur. Therefore genome integrity is lost and errors are susceptible to occur during transcription and translation processes. These can be responsible for cellular aging and cancers. Among the different DNA lesions that are known to be generated, many concern the nucleobases whose structures are depicted in Fig. 1. Despite many structural similarities – all of them being aromatic nitrogenated heterocycles – nucleobases show different susceptibilities to chemical or physical damaging agents. In order to find efficient ways to fight against the generation of DNA damage, it is fundamental on one hand to understand the mechanisms of formation of the different lesions that may be produced endogenously or exogenously in cellular DNA and, on the other hand, to be able to rationalize the differences of reactivity of the nucleobases toward a given genotoxic agent. The second aspect has been the subject of theoretical studies where the reactivity indexes presented in the previous section have been successfully applied to a number of cases [78–83]. Some of them will be described below with the aim of showing the wide range of reactivity issues that *conceptual DFT* can address.

In a first part, global and local reactivity indexes computed for the five main purine and pyrimidine nucleobases are gathered in the same place in order to have preliminary information on the differences between the nucleobases. The second

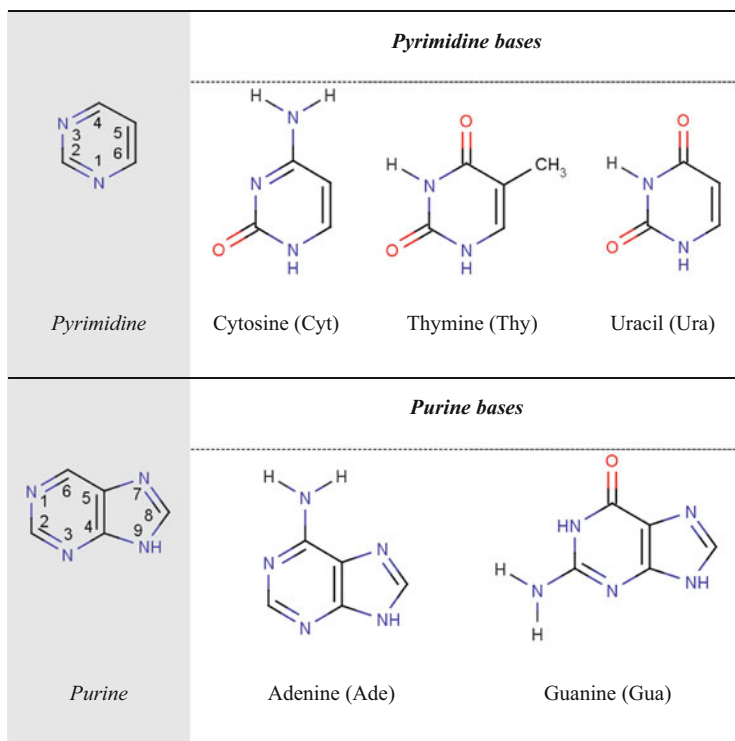


Fig. 1 Structure of DNA bases found in all living beings. Note that uracil is only present in RNA, contrary to thymine which is found in DNA only

part concentrates on information showing that reactivity descriptors can provide relevant structural features adopted by the nucleobases (base-pair formation, tautomers). Finally, the third and last part focuses, strictly speaking, on reactivity differences between the bases in the particular context of the formation of a given lesion.

3.2 *Reactivity Descriptors Computed for Isolated Nucleobases*

All the molecular properties have been computed through DFT methodology by using the B3LYP functional with the triple-zeta split valence basis set 6-311G(d,p). All the computations have been performed using the Gaussian package software [84]. The molecules have been fully optimized. Then the DFT-based descriptors have been calculated using the two usual sets of approximations, first the finite difference approximation, then the Koopmans' theorem. The latter approximation is questionable, especially for local indexes, but to our best knowledge, it has

always proved satisfactory for this kind of systems. Practically, the post calculations and condensations have been performed using the procedure proposed by Chamorro and Perez through their package “Global and Local Descriptor version 2.0” [85]. In this first part, the reactivity and selectivity descriptors of isolated bases are presented.

Global Indexes

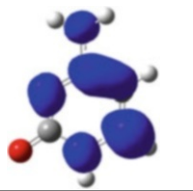
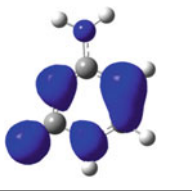
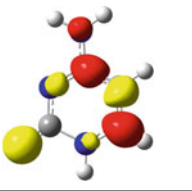
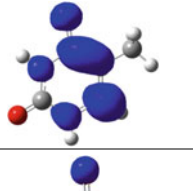
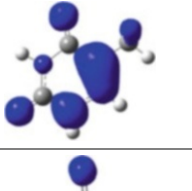
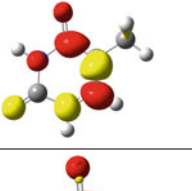
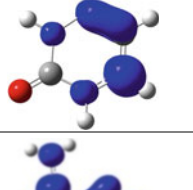
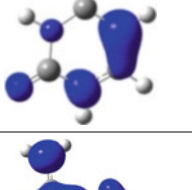
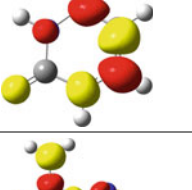
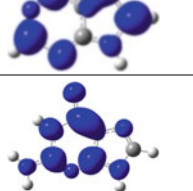
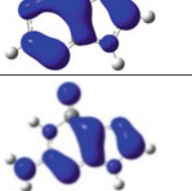
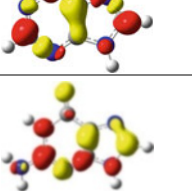
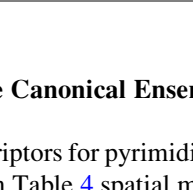
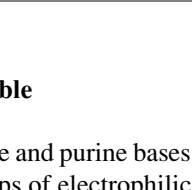
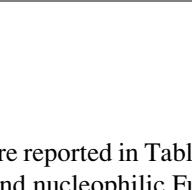
The global indexes calculated as stated above are gathered in Table 3. It is plain to note that the chemical potential (μ) of purine bases appears higher (less negative) than that of pyrimidine bases, making the former components better electron donors than the latter constituents. More precisely, Gua appears as the base which is the most easily oxidized, while Ura is the most resistant to oxidants. This is consistent with the fact that Gua is the preferential target in the formation of oxidatively generated damage at least when exposed to one-electron oxidants and singlet oxygen [18, 27]. In particular it can explain that usually Gua is the main target of ionization giving rise predominantly to 8-oxo-7,8-dihydroguanine (8-oxoGua) through the transient formation of the guanine radical cation either directly or after charge transfer from other one-electron oxidized nucleobases [18, 27, 86].

Besides, it is remarkable how close the hardness (η) of the five nucleobases are to each other (and thus their softness (S)), suggesting a similar resistance to charge transfer, though it can be noticed from comparison between Thy and Ura that methylation on C5 decreases the hardness by about 0.3 eV. Since the electrophilicity power is computed through ($\mu^2/2\eta$), the differences in electrophilicity power (ω) between the bases are mainly due to differences in their chemical potential. It appears that the purine bases are being better nucleophiles than the pyrimidine bases. Descriptors are also able to characterize the selectivity of molecules. This is the subject the next section focuses on.

Table 3 Global indexes computed from frontier orbitals at the B3LYP/6-311G(d,p) level

Bases		Canonical ensemble		Grand canonical ensemble		Other
		First order	Second order	First order	Second order	
		μ (eV)	η (eV)	N	S (eV ⁻¹)	
Pyrimidines	Cyt	−3.70	5.38	58	0.186	1.28
	Thy	−4.16	5.39	66	0.185	1.60
	Ura	−4.26	5.70	58	0.175	1.59
Purines	Ade	−3.40	5.44	70	0.184	1.06
	Gua	−3.33	4.58	78	0.179	1.20

Table 4 Local reactivity indexes computed from frontier orbitals at B3LYP/6-311G(d,p) level

Base		Second order		Third order
		$f^+(r)$	$f^-(r)$	$\Delta f(r)$
		Electrophilic sites	Nucleophilic sites	Red: more E than Nu Yellow: more Nu than E
Pyrimidine	Cyt			
	Thy			
	Ura			
Purine	Ade			
	Gua			

Local Indexes of the Canonical Ensemble

Local reactivity descriptors for pyrimidine and purine bases are reported in Tables 4 and 5. Specifically, in Table 4 spatial maps of electrophilic and nucleophilic Fukui functions along with dual descriptor are displayed, while in Table 5 the corresponding condensed values are given. From a general point of view, it can be noted that spatial maps of Fukui functions are not very conclusive, while the tabulated data are more useful. Indeed the most reactive site, with respect to either an electrophile or a nucleophile, is respectively obtained by looking at the highest value of the electrophilic or nucleophilic Fukui function. On the contrary, since the sign of the dual descriptor carries information about the chemical philicity (electrophilicity/nucleophilicity), the maps are very often self-sufficient for rationalizing the chemical selectivity.

Table 5 Local reactivity indexes of pyrimidine and purine bases condensed through Chamorro and Perez scheme

Pyrimidine bases	Cytosine	Atom number	f_k^+	f_k^-	Δf_k
		N1	0.112	0.157	-0.045
		C2	0.007	0.015	-0.007
		N3	0.127	0.176	-0.049
		C4	0.190	0.007	0.183
		C5	0.097	0.262	-0.164
		C6	0.393	0.067	0.326
		N4 exo	0.001	0.002	-0.001
	Thymine	Atom number	f_k^+	f_k^-	Δf_k
		N1	0.056	0.231	-0.175
		C2	0.014	0.010	0.003
		N3	0.061	0.002	0.060
		C4	0.185	0.008	0.177
		C5	0.158	0.331	-0.173
		C6	0.381	0.149	0.233
		O4 exo	0.122	0.085	0.037
	Uracil	Atom number	f_k^+	f_k^-	Δf_k
		N1	0.059	0.253	-0.194
		C2	0.019	0.009	0.010
		N3	0.059	0.000	0.059
		C4	0.160	0.006	0.154
		C5	0.171	0.375	-0.204
		C6	0.399	0.123	0.276
		O4 exo	0.113	0.118	-0.006
Purine bases	Adenine	Atom number	f_k^+	f_k^-	Δf_k
		N1	0.126	0.149	-0.023
		C2	0.185	0.069	0.117
		N3	0.005	0.045	-0.040
		C4	0.211	0.067	0.144
		C5	0.036	0.159	-0.124
		C6	0.007	0.056	-0.050
		N7	0.073	0.060	0.013
		C8	0.246	0.121	0.126
		N9	0.038	0.015	0.024
	Guanine	Atom number	f_k^+	f_k^-	Δf_k
		N1	0.100	0.011	0.089
		C2	0.277	0.059	0.218
		N3	0.008	0.048	-0.040
		C4	0.192	0.112	0.080
		C5	0.110	0.220	-0.110
		C6	0.044	0.017	0.027
		N7	0.008	0.048	-0.040
		C8	0.028	0.175	-0.147
		N9	0.070	0.004	0.066

Pyrimidine Bases

The substantial contribution of C5 and C6 carbons of pyrimidine bases to the $f^+(r)$ and $f^-(r)$ descriptors indicates that the C5–C6 double bond of the pyrimidine ring is susceptible to both nucleophilic and electrophilic attacks. Nonetheless, the sign of the dual descriptor $\Delta f(r)$ indicates that carbon C5 is more nucleophilic than electrophilic ($\Delta f(r) < 0$), while this is the reverse for carbon C6 ($\Delta f(r) > 0$). Thus, an electrophile will add more efficiently to carbon C5 than to carbon C6, contrary to a nucleophilic reagent which will add more rapidly to carbon C6. This is consistent with the fact that the electrophilic $\cdot\text{OH}$, which is responsible for the majority of oxidatively generated damage to DNA, adds preferentially to carbon C5 of pyrimidine bases compared to carbon C6 [87]. It may be pointed out that $\cdot\text{OH}$ addition to the 5,6-pyrimidine double bond is under kinetic control since several computational studies have shown that addition to carbon C6 leads to a more stable adduct than addition to carbon C5 [88, 89].

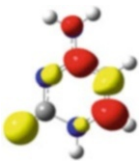
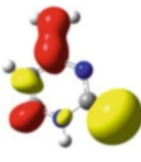
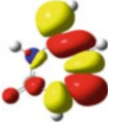

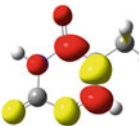
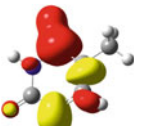
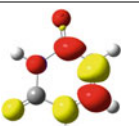
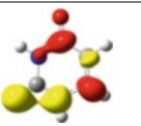
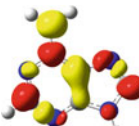
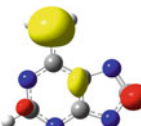
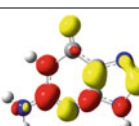
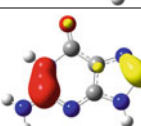
It is well documented that Cyt, Ade, and Gua may spontaneously deaminate through hydrolysis. Carbons holding the corresponding amino groups (C4 of Cyt, C6 of Ade, and C2 of Gua) all exhibit an electrophilic character. It will be shown in the following, in the particular case of Cyt (vide infra), that the reaction mechanism associated with spontaneous deamination reactions involves nucleophilic addition of a water molecule to those carbons (see Sect. 3.4).

Another well-documented fact is the chemical stability of the urea moiety of pyrimidine bases. Thus, position C2 is almost insensitive to both electrophiles and nucleophiles. All the selectivity indexes corroborate this statement for each pyrimidine base. As can be seen in Tables 4 and 5, neither the electrophilic nor the nucleophilic Fukui function exhibits significant values on C2. It is even clearer using the dual descriptor for which the value on C2 is roughly seven times lower than that of the other carbons.

Purine Bases

The most striking feature of purine bases is that two carbons of the 5-membered imidazole ring of the purine bases exhibit a different sign of the dual descriptor $\Delta f(r)$. C4 of Ade is nucleophilic only (almost zero contribution to $f^+(r)$), while that of Gua shows both nucleophilic and electrophilic characters (nonzero contribution to $f^+(r)$ and $f^-(r)$), the latter prevailing on the former. This is exactly the reverse for carbon C8 which corresponds to a pure nucleophilic site in Gua and to a nucleophilic and electrophilic site in Ade though more electrophilic than nucleophilic. In the following this difference in reactivity of the C8 carbon of purine bases is proposed to participate in the difference of reactivity of Gua and Ade toward the formation of tandem lesions in oxygen-free aqueous solution when DNA is exposed to $\cdot\text{OH}$ generated by radiolysis (see Sect. 3.4).

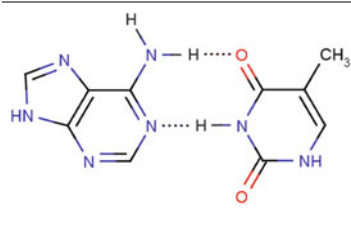
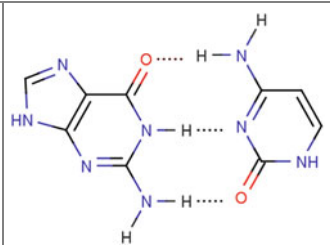
Table 6 Comparison of the dual descriptor and the dual potential computed from frontier orbitals at B3LYP/6-311G(d,p) level

Bases		Ground state	First excited state
		$\Delta f(r)$	$V^{\Delta f}(r)$
		Red: more E than Nu	Red: more Nu than E
		Yellow: more Nu than E	Yellow: more E than Nu
Pyrimidines	Cyt (canonical)		
	Cyt (imino tautomer)		
	Thy		
	Ura		
Purines	Ade		
	Gua		

First Excited State

Finally, the latter section deals with the preliminary information that can be extracted from indexes describing excited states. As already explained in Sect. 2.4, it can be inferred from the sign of the dual descriptor and that of the dual potential (see Table 6) that the nucleophilicity/electrophilicity excess of the reactive sites of the nucleobases is reversed when moving from the ground state to the first excited state of a base. As a consequence, the chemical behavior toward a partner is reversed too: sites which most easily give electrons in the ground state

Table 7 Watson-Crick base pairs

	
AT base pair	GC base pair

most favorably accept electrons in the first excited state and vice versa. We will see that this plays an important role in the regioselectivity observed in the formation of pyrimidine dimers when DNA is exposed to UVB radiation as discussed in Sect. 3.4.

3.3 Structural Features of DNA

The results presented so far deal only with isolated DNA bases in their ground and first excited states. In this context, they are only relevant for the test tube study of chemical reactions. Within biological environment, the chemical reactivity and selectivity of DNA bases may change. For instance, what is the impact of pyrimidine-purine hydrogen bond coupling? Besides, the influence of DNA backbone and chemical environment may modify the relative contribution of the tautomers. In this section, some interesting results regarding the role of such factors upon the chemical behavior of DNA bases are presented.

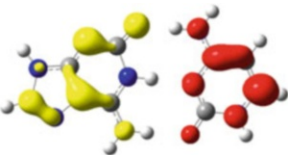
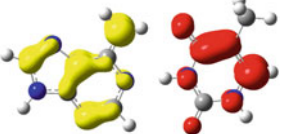
Formation of Base Pairs

The influence of the hydrogen bonding on the reactivity of DNA and RNA bases has been recently investigated by Toro-Labbé et al. [90] (Table 7). Their computation has been reproduced using B3LYP/6-311G(d,p) level of theory. The results are given in Tables 8 and 9. It appears that both the global and local reactivity are affected by the base pairing. Both chemical potential and hardness are of general lower value. The lowering of chemical potential signifies that, once paired, the bases are more easily excited and ionized. They are also more prone to react as their global hardness decreases. The local selectivity is also widely modified since it appears from the dual descriptor maps that electrophilic and nucleophilic sites are gathered on only one base. As it can be seen in Table 9, purine bases muster all the nucleophilic sites, while pyrimidine bases gather the electrophilic sites.

Table 8 Watson-Crick base pairs global descriptors computed from frontier orbitals at B3LYP/6-311G(d,p) level

		Canonical ensemble		Grand canonical ensemble		Other
		First order	Second order	First order	Second order	
DNA base pairs		μ (eV)	η (eV)	N	S (eV ⁻¹)	ω (eV)
Ade	Thy	-3.57	4.87	136	0.20	1.30
Gua	Cyt	-3.28	3.74	136	0.27	1.45

Table 9 Watson-Crick base pairs dual descriptor maps computed from frontier orbitals

DNA base pairs	$\Delta f(r)$
	Red: more E than Nu
	Yellow: more Nu than E
Guanine-cytosine	
Adenine-thymine	

It is also interesting to compare the two base pairs. The couple Ade-Thy has a lower chemical potential than that of Gua-Cyt, which means that the latter is more easily ionized for generating a radical cation. As already discussed, nucleophilic zones are mainly located on the purine moieties. Therefore the generated radical is also very likely to be located on the purine bases. The couple Gua-Cyt also has a lower hardness and therefore is more prone to undergo chemical reactions than the couple Ade-Thy. From this investigation, two main conclusions can be drawn. First, the effect of pairing can be rather important upon selectivity; the meaning of the dual descriptor between two species in interaction might be questionable though. Second, the couple Gua-Cyt is more reactive than the couple Ade-Thy.

Tautomerism

It is generally assumed that DNA bases do not possess tautomers at neutral pH and that they are always present in DNA in their canonical forms (see Table 10). However, numerous tautomers can be built by modifying the position of a hydrogen atom (prototropy). An example is given for cytosine for which four tautomers are easily identified. Chemical potential, hardness, and electrophilicity values for each of the tautomers are given in Table 11. As can be seen in Table 11, the hydrogen shift mildly modifies the chemical reactivity. The chemical potential varies of about

Table 10 Different forms of cytosine along with dual descriptor maps computed from frontier orbitals at B3LYP/6-311G(d,p) level

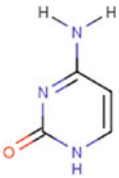
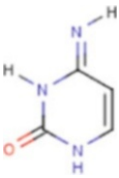
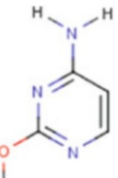
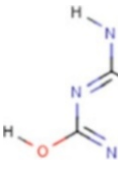
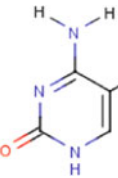
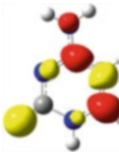
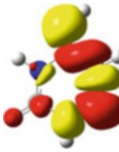
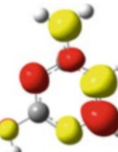
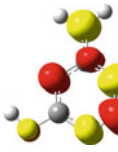
Cytosine				5-Methylcytosine
				
(1)	(2)	(3)	(4)	
Canonic	Tautomers			Methylated (epigenetic mark)
				$\Delta f(r)$

Table 11 Chemical potential, hardness, and electrophilicity values for the main tautomers of cytosine computed from frontier orbitals at B3LYP/6-311G(d,p) level

Numbering		μ (eV)	η (eV)	ω (eV)	Rel. E_{tot} (kJ/mol)
(1)	Cyt – amino/oxo	−3.70	5.38	1.28	0.0
(2)	Cyt – imino/oxo	−3.80	5.41	1.34	+4.5
(3)	Cyt – amino/enol – 1	−3.56	5.81	1.09	+3.3
(4)	Cyt – amino/enol – 2	−3.57	5.80	1.10	+6.6

0.25 eV. The variations of chemical hardness are larger than that of chemical potential and go up to 0.40 eV.

From the local point of view, it is worth noticing that the exocyclic N4 atom of the amino group is predicted as a nucleophile for all the tautomers, while for the canonical form it is proposed to be electrophile. This modification of the local reactivity has proved to be useful for understanding the occurrence of pyrimidine dimer lesions (see Sect. 3.4).

3.4 Reactivity Differences Between the Nucleobases

As mentioned earlier, experimentalists have identified many examples where the nucleobases show differences in the susceptibility to a given genotoxic agent/environment, for example, because they measured different rate constants associated with the formation of a transient damage, or because they observed different regioselectivities associated with a given set of experimental conditions. In those

cases where the lesion is formed under kinetic control, conceptual DFT reactivity descriptors can be helpful in providing rationalizing elements. As the nucleobases have different numbers of electrons (see Table 3), responses of the grand canonical potential are expected to be the relevant reactivity descriptors to analyze for this purpose. The spontaneous deamination of cytosine and its derivatives will be used to illustrate how such an approach can allow quantifying differences of reactivity.

Nonetheless, it will be shown beforehand that the consideration of the dual character of some reactivity descriptors of the canonical example can give useful information as long as one is interested by qualitative differences in reactivity. This will be illustrated through two examples: one lesion formed on the electronic ground state potential energy surface and another lesion involving a base in an electronic excited state.

Qualitative Differences of Reactivity

In the Ground State: Exploiting the Dual Descriptor

When DNA is exposed to ionizing radiation, surrounding water molecules are subject to radiolysis with the subsequent generation, among several reactive oxygen species (ROS), of highly reactive $\cdot\text{OH}$ [91]. The latter ROS is able to induce several types of oxidatively generated damage to DNA [18, 27]. Depending on the conditions, typically aerobic versus anaerobic, some lesions are specifically produced or their formation favored. In anaerobic conditions, a covalent link can be more efficiently formed between carbon C8 of a purine base and radicals issued from either its adjoining sugar moiety [40, 41] or the methyl group of an adjacent Thy [19, 39]. Though both purine bases can be involved in the formation of these lesions, Gua is experimentally observed to be more susceptible than Ade [92–94].

The general reaction mechanism proposed for the formation of these lesions involving Gua is shown in Fig. 2. The first step involves $\cdot\text{OH}$ -mediated hydrogen atom abstraction from either the sugar moiety of Gua or the methyl group of a Thy, leading to the formation of an electrophilic $\text{RR}'\text{CH}_2\cdot$ or $\text{RR}'\text{R}''\text{CH}\cdot$ radical. Subsequently, the carbon-centered radical thus formed adds to carbon C8 of the purine base by electrophilic radical addition. $\text{H}\cdot$ abstraction by a radical from the environment or through the implication of O_2 in aerated solutions [40] finally leads to the formation of the tandem lesion.

This mechanism has been studied computationally by DFT in the cases of Gua and Ade [95–97].

For both types of lesions (cdG/cdA and $\text{G}^{\wedge}\text{T}/\text{A}^{\wedge}\text{T}$), the electrophilic radical addition to C8 appears to be responsible for the difference of reactivity observed between the two purine bases. Computed activation energies associated with this radical step are reported in Table 12.

First, from the point of view of the relative global reactivity of the purine bases, since the chemical potential of Gua is higher than that of Ade (see Table 3), an electrophilic addition to Gua is expected to be less destabilizing (lower activation

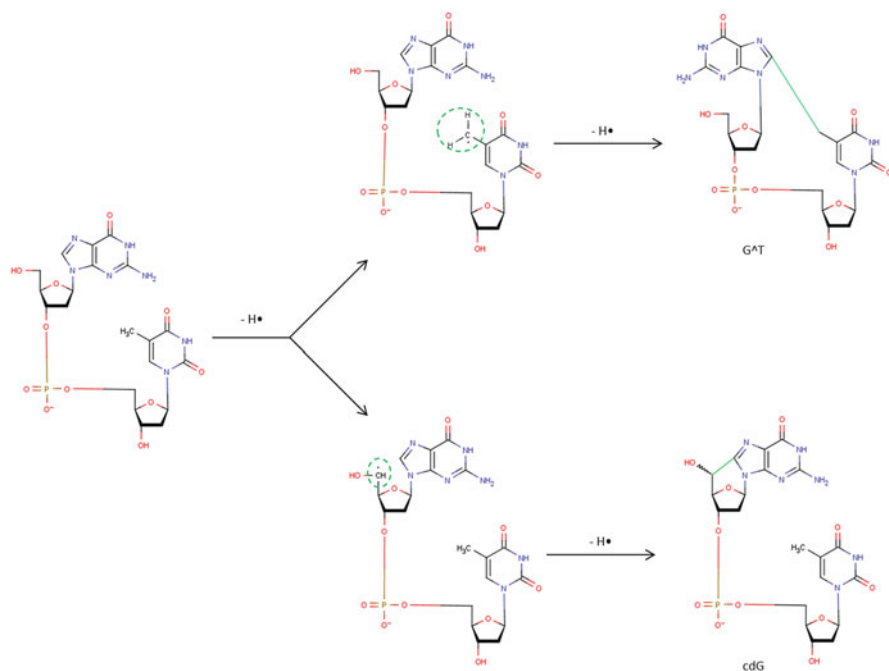


Fig. 2 Reaction scheme for the formation of cross-linked adducts between a purine base and either an adjacent thymine (G^T) or its sugar moiety (cdG)

Table 12 Activation energies (in kJ/mol) computed by DFT for the radical addition step leading to the formation of the tandem lesions sketched in Fig. 2

Lesion	$\Delta^\ddagger E$ (ZPE included)	Computational methodology	Reference
G^T	72.3	B3LYP/6-31G(d,p)	Xerri et al. [96], Labet et al. [98]
A^T	173.5		
cdG	41.0	B3LYP/6-31 + G(d,p)	Zhang and Eriksson [95]
cdA	55.2		

barrier) than to Ade. In addition, from a more local point of view, as we mentioned earlier, the two purine bases are characterized by different signs of the dual descriptor $\Delta f\left(\vec{r}\right)$ in the region of their C8 carbon, the site of addition during the formation of the tandem lesions. Thus, though both nucleophilic, the C8 carbons of the two purine bases are qualitatively different: carbon C8 of Gua is more nucleophilic than electrophilic ($\Delta f(r) < 0$), while carbon C8 of Ade is more electrophilic than nucleophilic ($\Delta f(r) > 0$) (see Table 4).

Now the dual descriptor $\Delta f(r)$ has been shown to be closely related to the maximum hardness principle [72]. When an electrophile approaches a nucleophile in a region characterized by $\Delta f(r) < 0$, then the hardness of the nucleophile is expected to increase, which is favorable. On the contrary, if the electrophile attacks the nucleophile on a reaction site characterized by $\Delta f(r) > 0$, the hardness of the nucleophile decreases, which is unfavorable.

As a conclusion, from both a global and local reactivity points of view, Gua is expected to be more susceptible than Ade to an electrophilic attack on its carbon C8. This explains the different formation yields experimentally observed between the purine bases for the tandem lesions reported in Fig. 2.

In an Excited State: Exploiting the Dual Potential

When DNA is exposed to UVB radiation (290–320 nm), the nucleobases can get electronically excited, thus allowing photochemical reactions to take place. Covalent links between two adjacent nucleobases can then be formed [32]. This is particularly frequent at bipyrimidine sites, i.e., when two pyrimidine bases are adjacent on the same DNA strand. As mentioned previously, the resulting photocycloadducts are called pyrimidine dimers. They are of two kinds: *i*) *cis-syn* cyclobutane pyrimidine dimers (CPDs) resulting from the [2 + 2] photocycloaddition between the C5 and C6 double bonds of two adjacent pyrimidine bases and *ii*) pyrimidine (6–4) pyrimidone photoproducts (6-4PPs) resulting from a Paternò-Büchi [2 + 2] photocycloaddition between the C5 and C6 double bond of the 5'-end pyrimidine base and the exocyclic C4-O/C4-N bond of the 3'-end thymine/cytosine imino tautomer, followed by opening and rearrangement of the oxetane/azetidine ring. The two kinds of pyrimidine dimers involving two adjacent thymines are shown in Fig. 3.

A Regioselectivity Problem

The eight possible bipyrimidine lesions susceptible to be formed (two structural types of dimers – four different bipyrimidine sites) are produced in very different proportions as shown in Fig. 4 where the yields of formation of each photoproduct within isolated DNA exposed to UVB radiation are reported [99].

From the consideration of the formation yields, it can be noticed that at any given bipyrimidine site, CPDs are produced more efficiently than 6-4PPs. The effect is more pronounced when the 3'-end pyrimidine base is Thy. To rationalize this experimental finding, which is merely a regioselectivity issue, reactivity descriptors can be analyzed. This is indeed possible, despite the fact this concerns photochemical properties, because a local descriptor that is applicable to the first excited state (the dual potential presented in Sect. 2.4) is now available in addition to the “classical” dual descriptor available for the ground state.

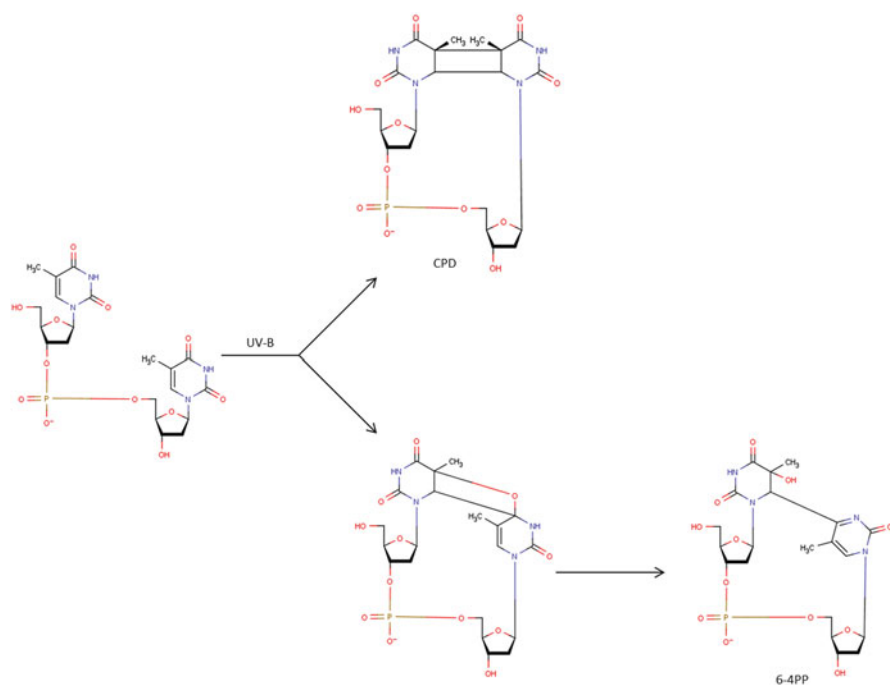


Fig. 3 Reaction scheme for the UV-induced formation of thymine dimers: cyclobutane pyrimidine dimer (CPD) and pyrimidine (6-4) pyrimidone photoproduct (6-4PP)

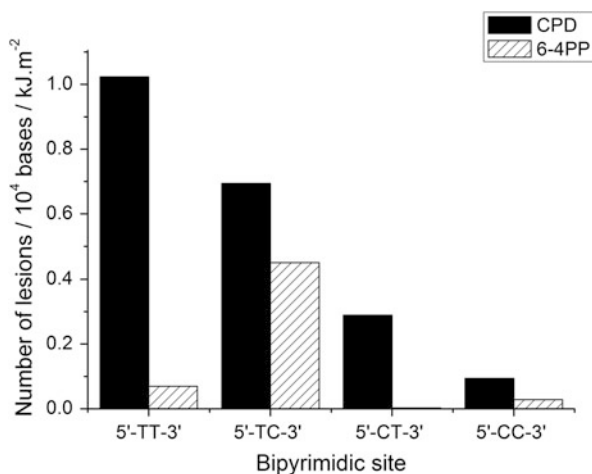


Fig. 4 Yield of formation of the main photoinduced bipyrimidine products within isolated DNA exposed to UVB radiation (dose range, 0–3.4 kJ·m⁻²) [99]

Table 13 Chemical behavior related to the sign of the dual descriptor for the ground state and the dual potential for the first excited state

Electronic state	Sign of the relevant descriptor	Chemical behavior
Ground state	$\Delta f(\vec{r}) > 0$	Electrophile
	$\Delta f(\vec{r}) < 0$	Nucleophile
First excited state	$V^{\Delta f}(\vec{r}) > 0$	Nucleophile
	$V^{\Delta f}(\vec{r}) < 0$	Electrophile

During the [2 + 2] photocycloadditions involved in both the formation of CPDs and 6-4PPs, one of the nucleobases is still in the ground state, while the other lies in the first excited state corresponding to the first $\pi \rightarrow \pi^*$ transition. Reaction between the two bases is all the more favorable because electrophilic sites of the excited base interact with nucleophilic sites of its partner and vice versa. As mentioned earlier and reminded in Table 13, the chemical behavior of reactive sites of the excited base is characterized by the sign of the dual potential $V^{\Delta f}(\vec{r})$; as for that of the reactive sites of the base in its ground state, it can be inferred from the sign of the dual descriptor $\Delta f(r)$. As a consequence interactions between a nucleophilic site of one base and an electrophilic site of the other base correspond to interactions between sites where the dual descriptor of one base and the dual potential of the other base are of the same sign.

About the Number of Stabilizing Interactions

Interacting sites are related to the pyrimidine dimer of interest. Formation of a CPD involves interaction between carbons C5 of both bases plus interaction between their carbons C6. The formation of a 6-4PP also involves two interactions: a first one between carbon C6 of the 5'-end base and carbon C4 of the 3'-end one and a second interaction between carbon C5 of the 5'-end base and O or N of the 3'-end base. In Fig. 5 the interactions that develop between the dual descriptor of the 5'-end base and the dual potential of the 3'-end base are shown for each of the eight potential photoadducts. Note that the fact to have considered the 3'-end base to be excited rather than the 5'-end one is purely arbitrary. Indeed, since the electrophilicity/nucleophilicity excess of the reactive sites is exactly reversed between the ground state and the first excited state (see Table 13), results would have been the same if we had considered the another alternative.

Since in a given electronic state the chemical behavior of C5 and C6 carbons is the same for Thy and Cyt and that this chemical behavior is reversed between the ground state and the first excited state, formation of CPDs systematically requires two stabilizing interactions, whatever the sequence of bases involved.

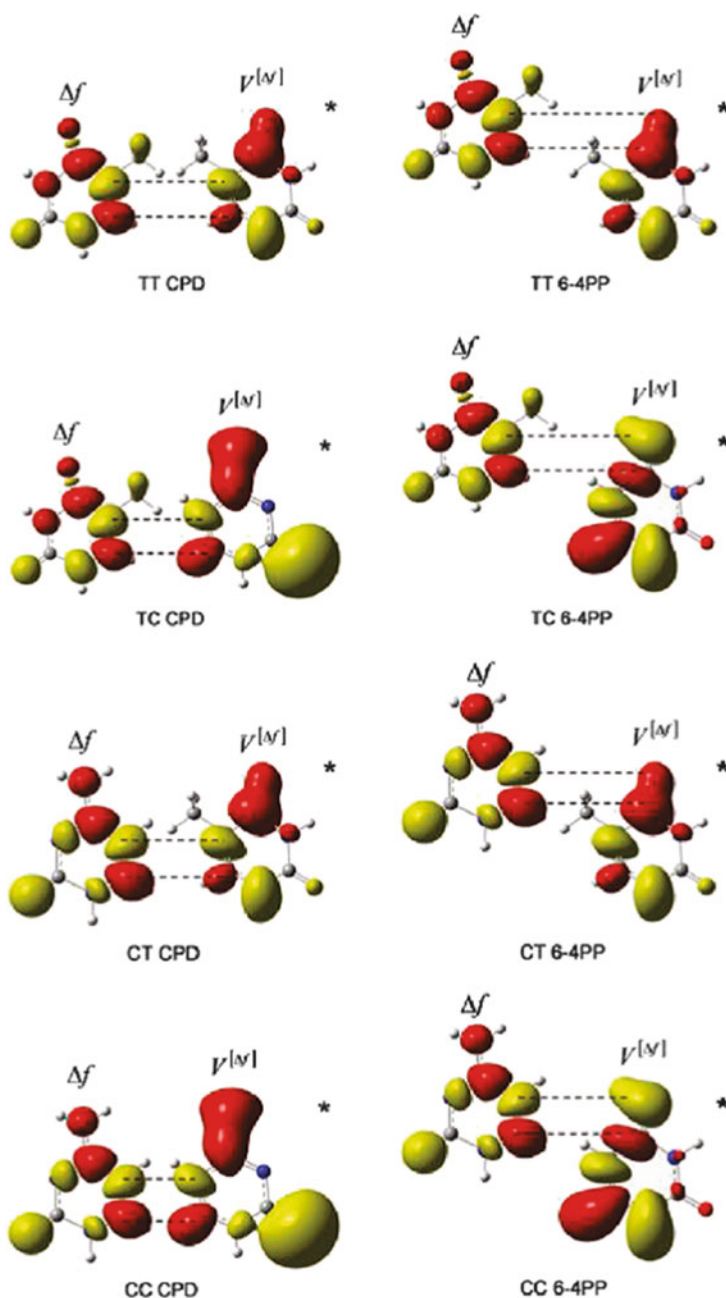


Fig. 5 Interactions at the four kinds of bipyrimidine sites between the dual descriptor of the 5'-end base in its ground state and the dual potential of the 3'-end base in its first excited state to form either a CPD or a 6-4PP lesion (Adapted from Ref. [76])

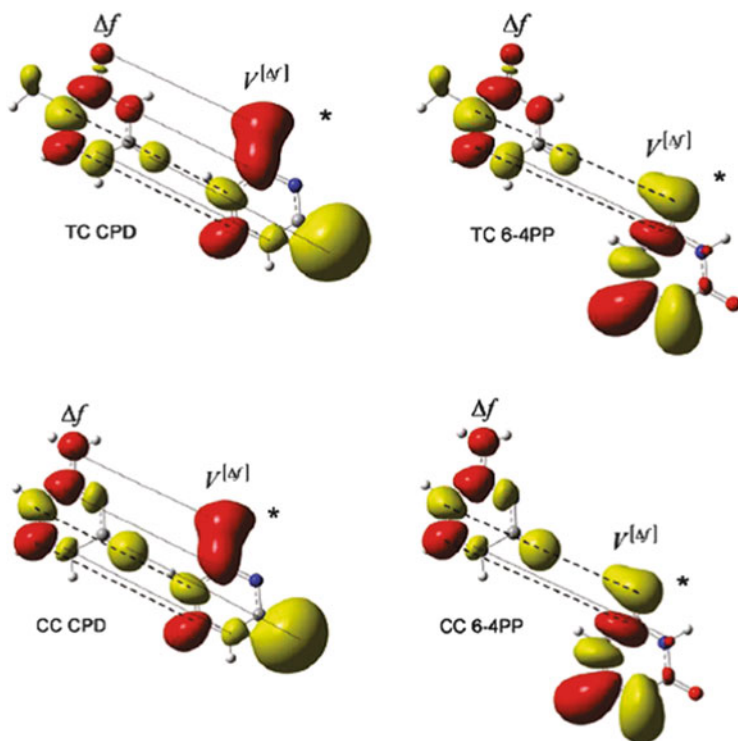


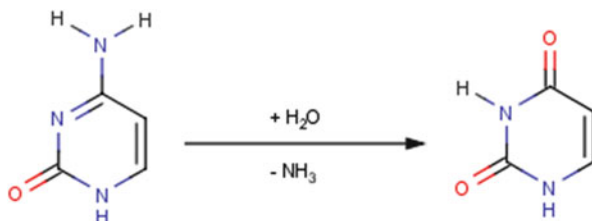
Fig. 6 Interactions at 5'-TC-3' and 5'-CC-3' bipyrimidine sites between the dual descriptor of the 5'-end pyrimidine base in its ground state and the dual potential of the 3'-end pyrimidine base in its first excited state to form either a CPD or a 6-4PP lesion. *Dashed lines* correspond to interactions leading to formation of the σ -bonds during the [2 + 2] photocycloaddition reaction. *Dotted lines* correspond to secondary interactions (Adapted from Ref. [76])

The formation of 6-4PPs, as shown in Fig. 5, involves two stabilizing interactions when a Cyt (in its imino form) constitutes the 3'-end base, but only one when this is a Thy. This is due to the fact that the oxygen linked to carbon C4 in Thy and the nitrogen linked to carbon C4 in the imino form of Cyt have reversed chemical behaviors. Therefore, the activation energy associated with the formation of a 6-4PP lesion is expected to be higher when a Thy base is at the 3'-end rather a Cyt. This explains why the formation of 6-4PP at 5'-TT-3' and 5'-CT-3' bipyrimidine sites is so inefficient compared to the corresponding CPDs.

About Secondary Interactions

The relative orientation of adjacent pyrimidine bases is governed by DNA double-stranded structure. Reacting bases approach each other in parallel planes (*supra-supra* approach). In addition to the interactions mentioned above which are

Fig. 7 Spontaneous cytosine deamination



responsible for the formation of two covalent links between adjacent pyrimidine bases, secondary interactions can develop. These are shown in Fig. 6 for the four dimers formed at bipyrimidine sites with 3'-end Cyt. The approach of pyrimidine bases to form 6-4PPs does not involve secondary interactions contrary to the approach giving rise to CPDs. In the latter case, four stabilizing secondary interactions develop (dotted lines in Fig. 6), facilitating the formation of CPDs compared to that of 6-4PPs, even in cases where the two primary interactions are stabilizing.

As a conclusion, the more efficient production of CPDs compared to 6-4PPs has two origins: (i) the number of stabilizing interactions responsible for the formation of covalent bonds between the two adjacent bases, which is 2 for all CPDs and 2 for 6-4PPs involving a 3'-end Cyt but only 1 for 6-4PPs involving a 3'-end Thy and (ii) the development of stabilizing secondary interactions during the formation of CPDs which do not exist in the case of 6-4PPs.

Quantitative Differences of Reactivity

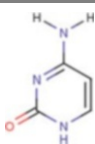
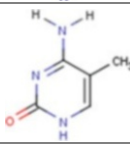
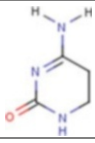
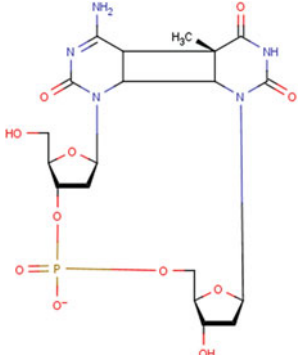
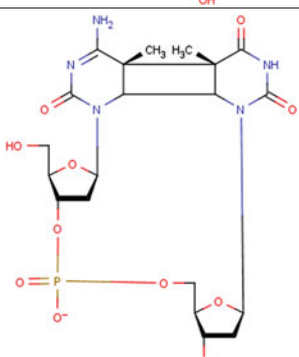
Exploiting the Grand Canonical Equivalent of the Dual Descriptor

Spontaneous Cyt deamination by hydrolysis occurs in living organisms. This hydrolytic reaction gives rise to Ura, the equation being shown in Fig. 7, whose abnormal presence in DNA is hopefully easily detected and removed by a dedicated repair enzyme.

Modified forms of canonical Cyt bases are also susceptible to deamination. This is, for example, the case of 5-methylcytosine and of 5,6-saturated derivatives of Cyt such as cytosine-containing pyrimidine dimers formed under UV radiation. These structural modifications affect strongly the deamination rate constants as reported in Table 14. Saturation of the C5–C6 bond accelerates considerably the deamination reaction. Incidentally, methylation at position 5 increases the deamination rate for 5,6-unsaturated cytosine derivatives, while it has exactly the opposite effect on 5,6-saturated derivatives.

A mechanism has been proposed and studied by DFT for cytosine deamination which is in agreement with the activation energy determined experimentally for the reaction (117 ± 4 kJ/mol [104]). The deamination pathway involves in a first step a nucleophilic addition of a water molecule to carbon C4 with the assistance of a second water molecule from the environment, followed by protonation of the amino

Table 14 Experimental deamination rate constant (k) of cytosine and some of its derivatives under various conditions

Bases	k	Experimental conditions	References
	$2.1 \times 10^{-10} \text{ s}^{-1}$	Single-stranded DNA pH = 7.4 – T = 37 °C	[100]
	$9.5 \times 10^{-10} \text{ s}^{-1}$	Single-stranded DNA pH = 7.4 – T = 37 °C	
	$6 \times 10^{-5} \text{ s}^{-1}$	Free base pH = 7.4 – T = 37 °C	[101]
	10^{-3} min^{-1}	Dinucleoside monophosphate pH = 7 – T = 25 °C	[102]
	10^{-5} min^{-1}	Dinucleoside monophosphate pH = 7 – T = 25 °C	

group and finally -NH_3 departure [98]. The same mechanism happens to hold for 5-methylcytosine deamination [105]. For 5,6-saturated derivatives, it appears that a tautomerization step leading to the imino form of the cytosine derivative is needed prior to the nucleophilic addition [106, 107]. In each case, the assisted nucleophilic

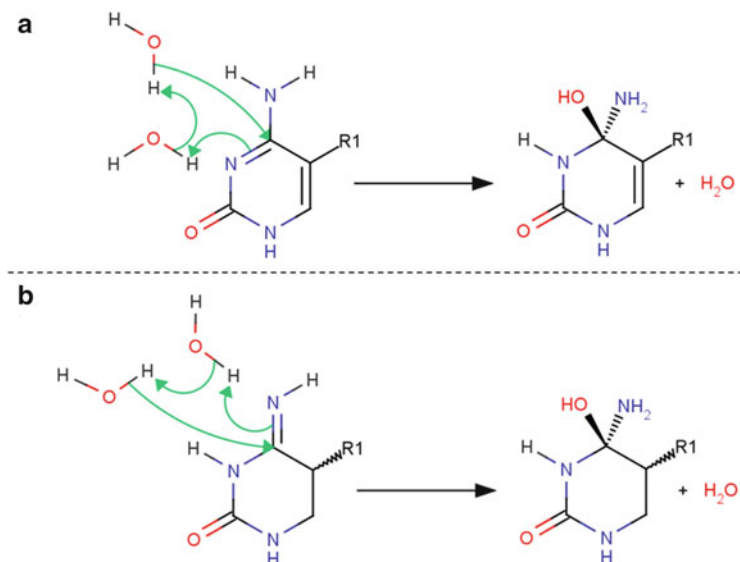


Fig. 8 Rate-controlling step of the mechanism proposed for deamination of 5,6-unsaturated (a) and 5,6-saturated (b) cytosine derivatives

addition, schematized in Fig. 8, has been identified as the rate-controlling step. It may be pointed out that the differences in the activation energies associated with this step for various investigated cytosine derivatives are in agreement with the deamination rate constants experimentally observed [107].

Since the nucleobases, either in their amino or imino form, constitute the reactant of the rate-determining step, the origin of the difference in sensitivity of the different forms of cytosine to the deamination reaction rate has to be searched among reactivity differences of the bases themselves, either global differences or local differences of their carbon C4 which undergoes the nucleophilic addition during the rate-determining step. In that purpose several global indexes and C4-local indexes computed for the different cytosine derivative are reported in Tables 15 and 16 respectively, both for the amino and imino forms of each base.

For 5,6-unsaturated forms of cytosine, methylation at position 5 tends to increase the chemical potential and to decrease, though only slightly for the imino form, the hardness. As a consequence the electrophilic power is quasi unchanged. It may be noted that this applies for both the amino and imino forms.

For 5,6-saturated forms of cytosine, methylation at position 5 has almost no effect, either on the chemical potential or on the hardness. And therefore this is also true for the electrophilic power. On the other hand, it has to be noted that 5,6-saturated derivatives of cytosine have higher chemical potentials than their 5,6-unsaturated counterparts and also much higher hardnesses, resulting in substantial lower electrophilic powers. This is in contradiction with the fact that methylation at position 5 and saturation of the C5–C6 bond both enhance the deamination

Table 15 Chemical potential, hardness, and electrophilic power of cytosine (Cyt), 5-methylcytosine (5mCyt), 5,6-dihydrocytosine (dhCyt), and 5,6-dihydro-5-methylcytosine (dh5mCyt) in their amino and imino tautomeric forms

Amino form				Imino form			
	μ (eV)	η (eV)	ω (eV)		μ (eV)	η (eV)	ω (eV)
Cyt	−3.70	5.38	1.28	Cyt	−3.80	5.41	1.34
5mCyt	−3.55	5.25	1.20	5mCyt	−3.67	5.38	1.25
dhCyt	−3.49	6.08	1.00	dhCyt	−3.56	6.72	0.94
dh5mCyt	−3.52	6.02	1.03	dh5mCyt	−3.60	6.82	0.95

Table 16 Electrostatic charge on carbon C4 (CHELPG method) [108] and grand canonical dual descriptor ($\frac{\Delta f_{C4}}{\eta^2}$ term) condensed (through *Chamorro and Perez scheme*) on carbon C4 for cytosine (Cyt), 5-methylcytosine (5mCyt), 5,6-dihydrocytosine (dhCyt), and 5,6-dihydro-5-methylcytosine (dh5mCyt) in their amino and imino tautomeric forms

Amino form			Imino form		
	q_{C4}	$\frac{\Delta f_{C4}}{\eta^2} (10^{-2} \text{ eV}^{-2})$		q_{C4}	$\frac{\Delta f_{C4}}{\eta^2} (10^{-2} \text{ eV}^{-2})$
Cyt	0.91	0.63	Cyt	0.73	0.29
5mCyt	0.74	0.73	5mCyt	0.63	0.40
dhCyt	0.86	1.03	dhCyt	0.65	0.61
dh5mCyt	0.70	1.02	dh5mCyt	0.56	0.58

rate. In conclusion, the difference in sensitivity of the different forms of cytosine to deamination must have a local origin.

Methylation at position 5 and saturation of the C5–C6 bond both tend to decrease the partial charge hold by carbon C4, indicating that the rate-controlling step is not under electrostatic control. Saturation of the C5–C6 double bond increases considerably the $\frac{\Delta f_{C4}}{\eta^2}$ value, in agreement with the fact that 5,6-saturated derivatives of cytosine undergo deamination much faster than the unsaturated forms.

As mentioned earlier, the grand canonical dual descriptor is a size consistent local index, suitable for comparing the reactivity of chemical systems of different sizes (as the different forms of cytosine) for a reaction under charge transfer control. This suggests that the nucleophilic addition of water to carbon C4 is under charge transfer control. This is supported by the fact that methylation at position 5 increases the value for 5,6-unsaturated forms of cytosine, while a decrease is observed for saturated compounds, in agreement with the effect of C5 methylation on the deamination reaction rate, which has opposite effects on saturated and unsaturated forms of cytosine.

Then, it can be concluded that the differences in sensitivity of the different forms of cytosine derivative to spontaneous deamination are closely related to modifications of the electrophilic power of their carbon C4 that is attacked during the reaction.

4 Conclusions

This chapter aims to review the use of DFT-based descriptors for understanding the chemical behavior of DNA bases. This approach can provide important information about the mechanism of formation of important DNA lesions and their occurrences. The usefulness of global DFT descriptors for investigating and predicting the reactivity of the bases is illustrated for several kinds of chemical situations. In parallel, local descriptors, specially the dual descriptor, help monitor the more reactive atomic sites within the bases. For instance, for the ground state, the dual descriptor gives a rationale for understanding the differences in reactivity of carbon C8 of adenine and guanine. Besides, the evolutions of the condensed values of the grand canonical dual descriptor of carbon C4 of Cyt derivatives clearly relate to the deamination rates of these compounds. Reactions between excited and ground state molecules are investigated by combining the dual potential and the dual descriptor respectively. This model accounts for the difference in formation efficiency between the formations of pyrimidine dimers. A general conclusion can be drawn from these investigations. Basically, the use of conceptual DFT descriptors is particularly efficient to explain qualitative differences of reactivity and selectivity between molecules, while quantum computations provide precise information but solely for a very specific set of chemical reagents. For an overall picture of a chemical reaction, it is interesting to combine the use of quantitative (computational reactivity studies) and qualitative (conceptual DFT approach) methods.

Acknowledgments All the authors thank INSERM: “This research has benefited from ITMO cancer of Aviesan within the framework Plan Cancer 2009–2013.” Cette recherche a bénéficié de l’aide de l’ITMO cancer d’Aviesan dans le cadre du Plan Cancer 2009–2013.

References

1. Lindahl T (1993) *Nature* 362:709–715
2. Cadet J (1994) In: Hemminki K, Dipple A, Shuker DEG, Kadlubar FF, Segerbäck D, Bartsch H (eds) DNA adducts, identification and biological significance. IARC Scientific Publication, Lyon, pp 125–245
3. Gentil A, Cabrak-Neto JB, Mariage-Samson R, Margot A, Imbach J-L, Rayner B, Sarasin A (1992) *J Mol Biol* 227:981
4. Carell T, Brandmayr C, Hienzsch A, Müller M, Pearson D, Reiter V, Thoma I, Thumbs P, Wagner M (2012) *Angew Chem Int Ed* 51:7110
5. Branco MR, Ficiz G, Reik W (2012) *Nat Rev Genet* 13:7
6. Kkriacionis S, Heintz N (2009) *Science* 324:929
7. Tahliani M, Koh KP, Shen YH, Pastor WA, Bandukwala H, Brudno Y, Agarawal S, Iyer LM, Liu DR, Aravind L, Rao A (2009) *Science* 324:930
8. Shapiro R, Klein RS (1966) *Biochemistry* 5:2358
9. Lindahl T, Lindahl B (1974) *Biochemistry* 13:3405
10. Shen JC, Rideout WM III, Jones PA (1994) *Nucleic Acids Res* 22:972
11. Lindahl T (1982) *Ann Rev Biochem* 51:61

12. Neddermann P, Jiricny J (1993) *J Biol Chem* 268:21218
13. Cadet J, Loft S, Olinski R, Evans MD, Bialkowski K, Wagner JR, Dedon PC, Moeller P, Greenberg MM, Cooke MS (2012) *Free Radic Res* 46:367
14. Murphy MP (2009) *Biochem J* 417:1
15. Ferguson LR (2010) *Mutat Res* 690:3
16. Park JB (2003) *Exp Mol Med* 35:325
17. von Sonntag C (2006) *Free-radical-induced DNA damage and its repair – a chemical perspective*. Springer, Berlin/Heidelberg/New York
18. Cadet J, Douki T, Ravanat J-L (2010) *Free Radic Biol Med* 49:9–21
19. Cadet J, Ravanat J-L, TavernaPorro M, Menoni H, Angelov D (2012) *Cancer Lett* 327:5
20. Dedon PC (2008) *Chem Res Toxicol* 21:206
21. Cadet J, Wagner J-R (2013) *Cold Spring Harb Perspect Biol* 5:a012559
22. Beckman JS, Beckman TW, Chen J, Marshall PA, Freeman BA (1990) *Proc Natl Acad Sci U S A* 87:1620
23. Denicola A, Freeman BA, Trujillo M, Radi R (1996) *Arch Biochem Biophys* 333:49
24. Medinas DB, Cerchario G, Trindale DF, Augusto O (2007) *IUBMB Life* 59:255
25. Crean C, Uvaydov Y, Geacintov N, Shafirovich V (2008) *Nucleic Acids Res* 36:742
26. Perrier S, Hau J, Gasparutto D, Cadet J, Favier A, Ravanat J-L (2006) *J Am Chem Soc* 128:5703
27. Cadet J, Douki T, Ravanat J-L (2008) *Acc Chem Res* 41:1075
28. Madugundu GS, Wagner JR, Cadet J, Kropachev K, Yun BH, Geacintov NE, Shafirovich V (2013) *Chem Res Toxicol* 26:1031–1033
29. Cadet J, Ravanat J-L, Martinez GR, Medeiros MH, Di Mascio P (2006) *Photochem Photobiol* 82:1219
30. Epe B (2012) *Photochem Photobiol Sci* 11:98
31. Cadet J, Sage E, Douki T (2005) *Mutat Res* 571:3
32. Cadet J, Mouret S, Ravanat J-L, Douki T (2012) *Photochem Photobiol* 88:1048
33. Courdavault S, Baudouin C, Charveron M, Canghaiem B, Favier A, Cadet J, Douki T (2005) *DNA Repair (Amst)* 4:836
34. Wallace SS, Murphy DL, Sweasy JB (2012) *Cancer Lett* 327:73
35. Friedberg EC (2001) *Nat Rev Cancer* 1:22
36. Heil K, Pearson D, Carell T (2011) *Chem Soc Rev* 40:4271
37. Budden T, Bowden NA (2013) *Int J Mol Sci* 14:1132
38. Batista FZ, Kaina B, Menegheni R, Menck CFM (2009) *Mutat Res* 681:197
39. Wang Y (2008) *Chem Res Toxicol* 21:276
40. Belmadoui N, Boussicault F, Guerra M, Ravanat J-L, Chatgililoglu C, Cadet J (2010) *Org Biomol Chem* 8:3211
41. Chatgililoglu C, Ferreri C, Terzidis MA (2011) *Chem Soc Rev* 40:1368
42. Geerlings P, De Proft F, Langenaeker W (2003) *Chem Rev* 103:1793
43. Chermette H (1999) *J Comput Chem* 20:129
44. Ayers PW, Anderson JSM, Bartolotti JL (2005) *Int J Quantum Chem* 103:1793
45. Senet P (1996) *J Chem Phys* 105:6471
46. Parr RG, Donnelly RA, Levy M, Palke WE (1978) *J Chem Phys* 68:3801
47. Parr RG, Pearson RG (1983) *J Am Chem Soc* 105:7512
48. Parr RG, Yang W (1984) *J Am Chem Soc* 106:4049
49. Geerlings P, Sablon N, Fievez T, De Proft F (2010) *Abs Papers Am Chem Soc* 240:212
50. Fuentealba P, Parr RG (1991) *J Chem Phys* 94:5559
51. Morell C, Grand A, Toro-Labbé A, Chermette H (2013) *J Mol Model* 19:2893–2900
52. Iczkowski RP, Margrave JL (1961) *J Am Chem Soc* 83:3547
53. Mulliken RS (1934) *J Chem Phys* 2:782
54. Yang W, Parr RG (1985) *Proc Natl Acad Sci U S A* 82:6723
55. Pearson RG (1983) *J Am Chem Soc* 85:3533
56. Pearson RG (1987) *J Chem Educ* 64:561

57. Parr RG, Zhou Z (1993) *Acc Chem Res* 26:256
58. Parr R, von Szventpaly L, Liu S (1999) *J Am Chem Soc* 121:1992
59. Klopman G (1968) *J Am Chem Soc* 90:223
60. Salem L (1968) *J Am Chem Soc* 90:543
61. Fukui K (1957) *J Chem Phys* 27:1247
62. Fukui K (1987) *Science* 218:747
63. Yang W, Mortier WJ (1986) *J Am Chem Soc* 108:5708
64. Hocquet A, Toro-Labbé A, Chermette H (2004) *J Mol Struct (THEOCHEM)* 686:213
65. Cadet J, Grand A, Morell C, Letelier JR, Montcada JL, Toro-Labbé A (2002) *J Phys Chem A* 107:5334
66. Fievez T, Weckhuysen BM, De Proft F, Geerlings P (2009) *J Phys Chem C* 113:19905
67. Muya JT, De Proft F, Geerlings P, Nguyen MT, Ceulemans A (2011) *J Phys Chem A* 115:9609
68. Sablon N, De Proft F, Geerlings P (2010) *J Chem Phys Lett* 1:1228
69. Yang W, Cohen A, De Proft F, Geerlings P (2012) *J Chem Phys* 136:144110
70. Sablon N, De Proft P, Sola M, Geerlings P (2012) *Phys Chem Chem Phys* 14:3960
71. Morell C, Grand A, Toro-Labbé A (2005) *J Phys Chem A* 109:205
72. Morell C, Grand A, Toro-Labbé A (2006) *Chem Phys Lett* 425:342
73. Berkowitz M, Parr RG (1988) *J Chem Phys* 88:2554
74. Ayers PW, Morell C, De Proft F, Geerling P (2007) *Chem Eur J* 13:8240
75. Morell C, Labet V, Grand A, Ayers PW, Geerlings P, De Proft F, Chermette H (2009) *J Chem Theory Comput* 5:2274
76. Morell C, Labet V, Ayers PW, Genovese L, Grand A, Chermette H (2011) *J Phys Chem A* 115:8032
77. Tognetti V, Morell C, Ayers PW, Joubert L, Chermette H (2013) *Phys Chem Chem Phys* 15:14465–14475
78. Kumar V, Kishor S, Ramaniah LM (2012) *J Mol Model* 18:3969
79. Ciino P, Gomez-Paloma L, Barone V (2004) *J Org Chem* 69:7414
80. Sivanesan D, Subramanian V, Nair BU (2001) *J Mol Struct (THEOCHEM)* 544:123
81. Saha S, Wang F, MacNaughton JB, Moewes A, Chang DP (2008) *J Synchrotron Radiat* 15:151
82. Saha S, Roy RK (2007) *J Phys Chem B* 111:9664
83. Parthasarti R, Amutha R, Subramanian V, Nair BU, Ramasami T (2004) *J Phys Chem A* 108:3817
84. Frisch MJ, Trucks GW, Schlegel HB, Scuseria GE, Robb MA, Cheeseman JR, Scalmani G, Barone V, Mennucci B, Petersson GA, Nakatsuji H, Caricato M, Li X, Hratchian HP, Izmaylov AF, Bloino J, Zheng G, Sonnenberg JL, Hada M, Ehara M, Toyota K, Fukuda R, Hasegawa J, Ishida M, Nakajima T, Honda Y, Kitao O, Nakai H, Vreven T, Montgomery JA Jr, Peralta JE, Ogliaro F, Bearpark M, Heyd JJ, Brothers E, Kudin KN, Staroverov VN, Kobayashi R, Normand J, Raghavachari K, Rendell A, Burant JC, Iyengar SS, Tomasi J, Cossi M, Rega N, Millam JM, Klene M, Knox JE, Cross JB, Bakken V, Adamo C, Jaramillo J, Gomperts R, Stratmann RE, Yazyev O, Austin AJ, Cammi R, Pomelli C, Ochterski JW, Martin RL, Morokuma K, Zakrzewski VG, Voth GA, Salvador P, Dannenberg JJ, Dapprich S, Daniels AD, Farkas O, Foresman JB, Ortiz JV, Cioslowski J, Fox DJ (2009) *Gaussian 09, Revision A.02*. Gaussian, Wallingford
85. Chamorro E, Perez P (2005) *J Chem Phys* 123:114107
86. Box HC, Dawidzik JD, Budzinski EE (2001) *Free Radic Biol Med* 31:856
87. Cadet J, Berger M, Douki T, Ravanat J-L (1997) *Rev Physiol Biochem Pharmacol* 131:1
88. Grand A, Morell C, Labet V, Cadet J, Eriksson LA (2007) *J Phys Chem A* 111:8968–8972
89. Akin M (2010) *Thesis of the Georgia Institute of Technology*, Atlanta
90. Inostroza-Rivera R, Herrera B, Toro-Labbé A (2012) *Comput Theor Chem* 990:222
91. Wagner JR, Cadet J (2010) *Acc Chem Res* 43:564
92. Bellon S, Ravanat J-L, Gasparutto D, Cadet J (2002) *Chem Res Toxicol* 15:598

93. Dizdaroglu M, Jaruga P, Rodriguez H (2001) *Free Radic Biol Med* 30:774
94. Jaruga P, Birincioglu M, Rodriguez H, Dizdaroglu M (2001) *Biochemistry* 41:3703
95. Zhang RB, Eriksson LA (2006) *Chem Phys Lett* 417:303–308
96. Xerri B, Morell C, Grand A, Cadet J, Cimino P, Barone V (2006) *Org Biomol Chem* 4:3986–3992
97. Labet V, Morell C, Grand A, Cadet J, Cimino P, Barone V (2008) *Org Biomol Chem* 6:3300
98. Labet V, Grand A, Morell C, Cadet J, Eriksson LA (2008) *Theor Chem Acc* 120:429
99. Douki T, Cadet J (2001) *Biochemistry* 40:2495
100. Ehrlich M, Norris KF, Wang RY-H, Kuo KC, Gehrke CW (1986) *Biosci Rep* 6:387
101. Slae S, Shapiro R (1978) *J Org Chem* 43:1721
102. Douki T, Cadet J (1992) *J Photochem Photobiol B* 15:199
103. Douki T, Cadet J (1994) *Biochemistry* 33:11942
104. Frederico LA, Kunkel TA, Shaw BR (1990) *Biochemistry* 29:2532
105. Labet V, Morell C, Cadet J, Eriksson LA, Grand A (2009) *J Phys Chem A* 113:2524
106. Labet V, Morell C, Douki T, Cadet J, Eriksson LA, Grand A (2010) *J Phys Chem A* 114:1826
107. Grand A, Cadet J, Eriksson LA, Labet V, Jorge NL, Schreiber ML, Douki T, Morell C (2012) *Theor Chem Acc* 131:1187
108. Breneman CM, Wiberg KB (1990) *J Comp Chem* 11:361

Structure, Bonding and Reactivity of Heterocyclic
Compounds

De Proft, F.; Geerlings, P. (Eds.)

2014, IX, 191 p. 144 illus., 106 illus. in color., Hardcover

ISBN: 978-3-642-45148-5